The physics of brown dwarfs

1998 J. Phys.: Condens. Matter 10 11235

(http://iopscience.iop.org/0953-8984/10/49/013)

J. Phys.: Condens. Matter **10** (1998) 11235–11245. Printed in the UK PII: S0953-8984(98)95332-2

The physics of brown dwarfs

G Chabrier

Centre de Recherche Astrophysique de Lyon (UMR CNRS 5574), Ecole Normale Supérieure de Lyon, 69364 Lyon Cédex 07, France

Received 22 June 1998

Abstract. We briefly outline the physics underlying the mechanical and thermal properties of brown dwarfs, which characterize their interiors and their atmospheres. We mention the most recent improvements realized in the theory of brown dwarfs and the connection with experimental and observational tests of this theory.

1. Introduction

A general outline of the basic physics underlying the structure and the evolution of brown dwarfs (BD) can be found in reviews by Stevenson (1991) and Burrows and Liebert (1993). Important innovations have occurred in the field since then, one of the least negligible being the *discovery* of bona fide brown dwarfs (Rebolo *et al* 1995, Oppenheimer *et al* 1995). An increasing number of these objects have now been discovered, either as companions of stars, as members of young clusters or as free-floating objects in the Galactic field (Ruiz *et al* 1997, Delfosse *et al* 1997). On the other hand, the theory has improved substantially within the past few years and can now be confronted directly with observations and even with laboratory experiments, as will be shown below. It is thus important to reconsider the previous reviews in the light of this observational and theoretical progress and to update our knowledge of the structure and the evolution of BDs. This is the aim of the present article.

BDs are objects that are not massive enough to sustain hydrogen burning in their core and thus to reach thermal equilibrium, defined as $L = L_{nuc}$ where

$$L_{nuc} = \int_0^M \epsilon \, \mathrm{d}m$$

is the nuclear luminosity and ϵ is the nuclear reaction rate per unit mass. This hydrogen-burning minimum mass M_{HBMM} depends on the internal composition of the object, in particular the abundance (by mass) of helium (Y) and heavier elements (Z). For abundances characteristic of the solar composition, typical of the Galactic disc population, $Y_\odot = 0.27$ and $Z_\odot = 0.02$, this minimum mass is $M_{\mathrm{HBMM}} \sim 0.072\ M_\odot$, whereas for compositions characteristic of the Galactic halo ($Y = 0.25$, $Z \sim 10^{-2}\ Z_\odot$), $M_{\mathrm{HBMM}} \sim 0.083\ M_\odot$ (Chabrier and Baraffe 1997, Baraffe *et al* 1997) and, for the zero-metallicity limit ($Z = 0$), $M_{\mathrm{HBMM}} \sim 0.09\ M_\odot$ (Saumon *et al* 1994).

The minimum mass for BDs is at present undetermined and masses as small as a Jupiter mass ($10^{-3}\ M_\odot$) are not excluded in principle. The dividing line between BDs and giant planets (GPs) is still unclear and stems essentially from their formation processes:

0953-8984/98/4911235+11$19.50

hydrodynamic collapse of an interstellar molecular cloud for BDs, like for stars, accretion of heavy elements in a protostellar disc for the formation of planetesimals which eventually become dense enough to capture hydrogen and helium and form gaseous planets. The accretion scenario—as opposed to the collapse scenario—for the formation of planets is supported by the distinctly super-solar average abundance of heavy elements in Jupiter and Saturn, although there is only indirect evidence for the presence of the central rocky core through the modelling of the centrifugal moments. The borderline between these two scenarios is at present unknown and involves most probably complex dynamical and non-linear effects. Extra-solar planets with masses as large as $\sim$40 $M_{\rm J}$ and BDs with masses as low as $\sim$30 $M_{\rm J}$ have now been discovered. Except for this formation process and for the presence of a central rock/ice core, the physics and the observational signatures for BDs and GPs are very similar. Since a complete review has been devoted to GPs (Stevenson 1998), the present work will be devoted to BDs. In the present survey, I will focus on the most recent improvements realized in the physics of the interior and the atmosphere of BDs. I will also mention the physics underlying the so-called lithium test, which provides a powerful independent way of establishing the sub-stellar nature and the age of a putative BD. The aim of the present paper is not to present detailed calculations (which can be found in the various references mentioned) but rather to capture the physics underlying the structure and the evolution of BDs.

2. Interiors of brown dwarfs; the equation of state for hydrogen

The central conditions for massive BDs are typically $T_c \lesssim 10^5$ K and $\rho_c \sim 10^2$–10^3 g cm^{-3}. Under these conditions, the average ion electrostatic energy $(Ze^2)/a$, where

$$a = \left(\frac{3}{4\pi}\frac{V}{N_i}\right)^{1/3}$$

is the mean inter-ionic distance, is several times the average kinetic energy kT, characterizing a strongly coupled ionic plasma with a coupling parameter $\Gamma_i = (Ze)^2/akT > 1$. The temperature is of the order of the electron Fermi temperature kT_F and the average inter-electronic distance a_e is of the order of both the Bohr radius, $a_e \sim a_0$, and the Thomas–Fermi screening length, $a_e \sim a_{TF}$. We thus have to deal with a partially degenerate, strongly correlated, polarizable electron fluid. The temperature in the envelope is $kT \lesssim 1$ Ryd, so we expect electronic and atomic recombination to take place. Finally, the electron average binding energy is of the order of the Fermi energy, $Ze^2/a_0 \sim \epsilon_F$, so *pressure* ionization is taking place along the internal density profile.

Recently, laser-driven shock-wave experiments have been conducted at Livermore (Da Silva *et al* 1997, Collins *et al* 1998) which directly probe the thermodynamic properties of dense hydrogen under conditions characteristic of BDs and GPs. The relevance of the Livermore experiments for the interior of these objects can be grasped from figure 1. About a decade ago, Saumon and Chabrier (1991, 1992; SC) developed a free-energy model aimed at describing the thermodynamic properties of strongly interacting H_2 molecules, H atoms, H^+ protons and electrons under such astrophysical conditions. The abundances of each species derive from the free-energy minimization:

$$\delta F(N_{\rm H_2}, N_{\rm H}, N_{\rm H^+}, N_{\rm e^-}, V, T) = \sum_i \frac{\partial F}{\partial N_i}\delta N_i = 0. \qquad (1)$$

This model relies on the so-called chemical picture, which assumes that the species remain distinct even at high density. This requires the knowledge of the inter-particle

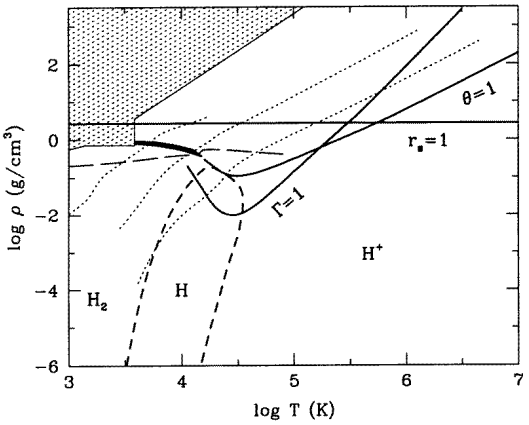

Figure 1. The phase diagram of hydrogen in the $T-\rho$ plane. The coexistence curve of the plasma phase transition (PPT) appears to the left of centre as a black solid line which ends at the critical point. Curves of constant ionic (Γ) and electronic (r_s) plasma coupling parameter and electron degeneracy parameter $\theta = T/T_F$ are shown. Regions dominated by molecules, atoms and ionized H are labelled and delimited by a curve which corresponds to 50% dissociation and ionization. The calculated shock Hugoniot corresponding to the experiments is shown by the long-dash curve across the diagram. Finally, the thin dotted lines show the internal structure profiles of several astrophysical bodies (from left to right): Jupiter, a 7 Ga brown dwarf of mass 0.055 $M_\odot$ and a 0.1 $M_\odot$ star. The EOS model is invalid in the shaded region.

potentials $\phi_{H_2H_2}$, ϕ_{H_2H} and ϕ_{HH}. Since N-body effects strongly modify the interaction between particles at high density, 'effective' pair potentials can be derived from the experimental Hugoniots. These effective pair potentials mimic the softening of the interaction due to the surrounding particles and thus retain some density dependence in the characteristic interactions between the main species. At the time at which the SC formalism was derived, the only available shock-wave experiments were the ones by Nellis *et al* (1983). Since molecular dissociation was negligible under these conditions, only an effective potential between H_2 molecules could be derived. The H_2–H and H–H potentials were taken as *ab initio* potentials. The more recent experiments by Weir *et al* (1996) reach higher pressures, and substantial molecular dissociation is inferred from these experiments ($X_H > 20\%$). This allows us to derive effective potentials for $\phi_{H_2H_2}$ and ϕ_{H_2H} as well and thus to update the SC model.

The recent laser-driven experiments have shown that the agreement between the *predictions* of the SC model and the data is excellent. In particular, the strong compression factor arising from the hydrogen pressure dissociation and ionization observed in the experiment ($\rho/\rho_i \sim 5.8$) agrees well with the predicted theoretical value (Saumon *et al* 1998). The compression is slightly underestimated in the theory and starts at a slightly too large a pressure. This reflects the underestimated degree of dissociation in the model, which stems from the too repulsive (*ab initio*) ϕ_{H_2H} potentials at the time at which the SC model was elaborated. These shortcomings are resolved when including the aforementioned new effective H_2–H_2 and H_2–H potentials. Eventually, full ionization is reached at very high pressure ($P \sim 10$ Mbar), characterized by the asymptotic compression factor $\rho_f/\rho_i = 4$ for a monatomic fully dissociated proton fluid. These results show that, although this 'chemical' model certainly does not pretend to give an exact, complete description of all of the interactions in the high-pressure strongly correlated fluid, it very probably retains the

main physics underlying the phenomenon of pressure dissociation/ionization.

It is worth noting that a similar strong compression factor is obtained also with the so-called fugacity expansion scheme, which is in principle exact in the strongly dissociated regime (Rogers and Young 1997), although this scheme fails at lower density when substantial recombination occurs.

One of the most striking features of the SC theory is the prediction of a first-order so-called plasma phase transition (PPT) between a molecular state and a plasma state for the pressure ionization of hydrogen, similar to the one predicted originally by Wigner and Huntington (1935). However, it is important to stress that the PPT in the SC model arises from the first-principles thermodynamical instability of the one single free-energy model ($(\partial P/\partial \rho)_T < 0$) and not from a comparison between two different free-energy models. The new SC EOS, incorporating the new potentials, still predicts a PPT, although with a critical point slightly cooler than predicted previously, namely at $T_c = 14\,600$ K, $P_c = 0.73$ Mbar (Saumon *et al* 1998). In order to really 'nail down' the existence of the PPT, we have calculated a second-shock Hugoniot reflected from the principal one, which should be realizable in the near future (Saumon *et al* 1998). Such an experiment should confirm or rule out definitely the presence of a PPT.

The main question about the PPT is: if it exists, what is its nature? This question has been addressed to some extent by Saumon and Chabrier (1992). If the PPT exists, it stems very probably from the large difference between a molecular state characterized by a strongly repulsive potential and a plasma state characterized by a soft Yukawa-like potential. Given the large difference between these two potentials, and thus the respective available phase spaces, we can expect a discontinuity in the interaction energy and thus an abrupt change in the two-particle distribution function. This behaviour is observed in recent path-integral Monte Carlo simulations (Magro *et al* 1996, Ceperley 1998). In terms of ground-state energies, this translates into the large energy barrier between the ground-state energy of an H_2-like system (H_2 or H_2^+) and an H^+-like system. In terms of correlation lengths that characterize the many-body effects, the system will collapse from a dense molecular phase characterized by a length $\lambda_{H_2} \sim$ a few a_0 into a plasma phase characterized by a length $\lambda_{H^+} \ll \lambda_{H_2}$. The underlying critical quantity will be the electron correlation length, with a critical percolation from a 'bound-electron'-like value to a 'free-electron'-like value. In this sense the PPT resembles the metal–insulator transition in metals associated with the liquid–vapour transition (Hensel 1998), leading eventually to a polarization catastrophe (Goldstein and Ashcroft 1985). The effect is likely to be more dramatic for hydrogen because of the absence of core electrons.

In this sense, the conductivity measurements of dense fluid hydrogen by Weir *et al* (1996) do not rule out a PPT. The conductivity exhibits a plateau with $\sigma \sim 2000\ \Omega^{-1}\ \mathrm{cm}^{-1}$ up to the highest pressure reached, $P \sim 1.8$ Mbar. This is still orders of magnitude smaller than the conductivity characteristic of a fully dissociated plasma phase, $\sigma \sim 10^5\ \Omega^{-1}\ \mathrm{cm}^{-1}$ (Stevenson and Ashcroft 1974) and is consistent with conduction being due to delocalized electrons from H_2^+. This does not preclude a *structural* transition like the PPT at higher pressures.

If the PPT exists it can have important consequences for BDs and GPs. The interiors of these objects are essentially isentropic. Since the signature of a first-order transition is a density and entropy discontinuity, integration along the internal adiabat from the observed outer conditions yields different central conditions with and without PPT (Chabrier *et al* 1992). In principle, the signature of a PPT in the interior of a GP like Jupiter and Saturn could be observed from the analysis of p-mode oscillations (Marley 1994, Gudkova *et al* 1995). However, this requires very accurate observations of high-degree modes, a difficult

observational task. The PPT also has important consequences for the evolution of these objects. Since by definition BDs and GPs do not sustain hydrogen burning, application of the first and second principles of thermodynamics yields the following equation for their evolution:

$$L = -\frac{\mathrm{d}}{\mathrm{d}t}\int_0^M \left(\tilde{u} + \frac{P}{\rho^2}\frac{\mathrm{d}\rho}{\mathrm{d}t}\right)\mathrm{d}m = -\int_0^M T\frac{\mathrm{d}\tilde{s}}{\mathrm{d}t}\,\mathrm{d}m \tag{2}$$

where L is the luminosity, $\tilde{u}$ and $\tilde{s}$ the specific internal energy and entropy, respectively. If the PPT exists, an additional term, namely the latent heat of the phase transition, must be added to the previous equation:

$$L' = L + \int_{\Delta m} T\frac{\mathrm{d}\,\Delta\tilde{S}}{\mathrm{d}t}\,\mathrm{d}m. \tag{3}$$

This effect was first pointed out by Stevenson and Salpeter (1977) and examined in detail by Saumon *et al* (1992).

3. The atmosphere of brown dwarfs

3.1. Spectral distribution

The photosphere is defined as the location where the photon mean free path is of the order of the mean inter-particle distance, i.e. $l_\nu \sim 1/(\bar{\kappa}\rho) \sim a \propto \rho^{-1/3}$, where $\bar{\kappa} \sim 1\ \mathrm{cm}^2/g$ is the mean absorption coefficient (opacity). This equality yields $l_\nu \sim a \sim 1$ cm. In terms of the dimensionless optical depth $\tau = z/l_\nu$, where z is the depth of the atmosphere, equilibrium between internal and gravitational pressure yields

$$\mathrm{d}\tau = -(\rho\bar{\kappa})\,\mathrm{d}z = \bar{\kappa}\,\frac{\mathrm{d}P}{g} \tag{4}$$

where $g = GM/R^2$ is the surface gravity. For BDs, $M \lesssim 0.1\ M_\odot$, $R \sim 0.1\ R_\odot$, $g \lesssim 10\ g_\odot$. This yields $P_{ph} \sim g/\bar{\kappa} \sim 10$ bar at the photosphere, and $\rho_{ph} \sim 10^{-5}$–10^{-4} g cm^{-3}. Collision effects are significant under these conditions. Therefore thermodynamic equilibrium can be safely assumed near the photosphere. The bad news is that collision effects can induce dipoles between molecules, e.g. H_2 or He–H_2, which otherwise would have only quadrupolar transitions. This so-called collision-induced absorption (CIA) between roto-vibrational states ($v \rightarrow v'$) of e.g. two H_2 molecules (1 and 2) can be written in terms of the two-body absorption (see, e.g., Borysow *et al* 1985):

$$\kappa_{\mathrm{H_2H_2}} = \sum_{v_1,v_1'}\sum_{v_2,v_2'} \alpha_{\mathrm{H_2H_2}}^{v_1,v_1',v_2,v_2'}(\omega, T) = n_{\mathrm{H_2}}^2\frac{2\pi^2}{3\hbar c}w(1-\mathrm{e}^{-\hbar\omega/kT})\sum_{v_1,v_1'}\sum_{v_2,v_2'} g^{v_1,v_1',v_2,v_2'}(\omega, T) \tag{5}$$

where $\omega = 2\pi\nu$ is the angular frequency, $n_{\mathrm{H_2}}$ is the number density of hydrogen molecules and $g^{v_1,v_1',v_2,v_2'}(\omega, T)$ is the spectral function. We note the dependence on the square of the number abundance. As temperature decreases below ~4000 K, an increasing number of hydrogen molecules form and thus H_2 CIA becomes overwhelmingly important, a feature shared with the atmospheres of giant planets and white dwarfs. Since the CIA of H_2 under the conditions of interest for BDs and GPs takes place at around 2.2 μm, energy conservation leads to a redistribution of the emergent radiative flux toward shorter wavelengths (Saumon *et al* 1994, Baraffe *et al* 1997).

The effective temperature is defined as the integral of the Eddington flux over the frequency spectrum:

$$T_{\rm eff}^4 = \sigma^{-1} \int H_\nu \, {\rm d}\nu \tag{6}$$

where $\sigma = 5.67 \times 10^{-5}$ erg cm^2 K^4 s^{-1} is the Stefan–Boltzmann constant. BDs are characterized by effective temperatures $T_{\rm eff} \lesssim 2000$ K. At these temperatures, numerous molecules such as H_2, H_2O, TiO and VO are stable and are the major absorbers of photons. These strongly frequency-dependent opacity sources yield a strong departure from a black-body energy distribution (see, e.g., figure 5 of Allard *et al* 1997). An updated detailed review of the physics of the atmosphere of low-mass stars and BDs is given by Allard *et al* (1997).

Below $T \sim 1800$ K, carbon monoxide, CO, is predicted to dissociate and to form methane, CH_4, as observed in Jupiter. This prediction has been confirmed by the discovery and the spectroscopic observation of Gliese229B. The presence of methane in its spectrum attested unambiguously to its sub-stellar nature. Consistent synthetic spectra and evolutionary calculations done by both the Lyon group (Allard *et al* 1996) and the Tucson group (Marley *et al* 1996) showed the mass of the object to be between ∼20 and 50 M_J, the indeterminacy in the mass reflecting the indeterminacy in the age of the system.

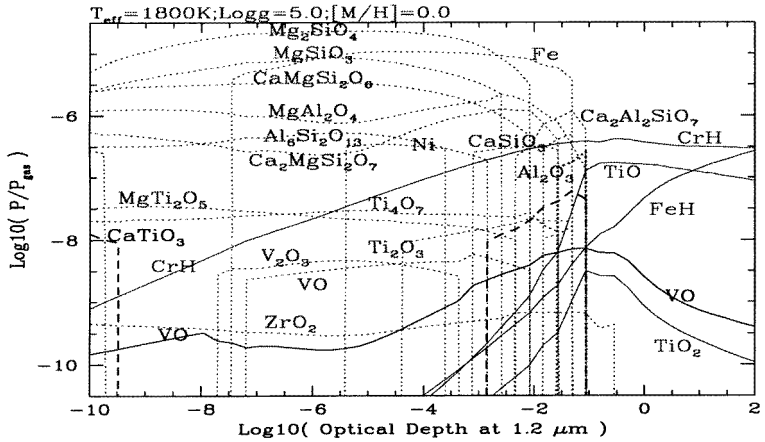

Figure 2. Relative abundances of gas-phase (full lines) and crystallized species (dotted lines) across a $T_{\rm eff} = 1800$ K brown dwarf model atmosphere (after F Allard).

Finally, below ∼2000 K, complex compounds (grains, also called 'clouds' by planetologists) condense in the atmosphere (see, e.g., Lunine *et al* 1986, Tsuji *et al* 1996). These grains will affect the atmosphere in different ways. They first modify the EOS itself and thus also the atmospheric temperature/density profile, and they also strongly affect the atmospheric opacity and thus also the emergent radiation spectrum. Finally, they will produce an increase of the temperature in the uppermost layers of the atmosphere, the so-called back-warming (or greenhouse) effect, destroying otherwise stable polyatomic species. The condensation of the grains in a BD atmosphere is illustrated in figure 2. Spectroscopic observations of different BDs at various effective temperatures show evidence for an even more complicated problem, namely grain diffusion (settling) in the atmosphere.

3.2. Energy transport

The radiative transport equation reads

$$F_{rad} = \frac{4}{3\bar{\kappa}\rho}\frac{\mathrm{d}}{\mathrm{d}r}(\sigma T^4) \propto \frac{\nabla T}{\bar{\kappa}} \tag{7}$$

for the radiative flux, while the convective transport can be written as

$$F_{conv} \propto (\rho v_{conv})(\tilde{c}_p\,\delta T) \tag{8}$$

where v_{conv} is the convection velocity, typically a fraction of the speed of sound, $\tilde{c}_p$ is the specific heat of the matter at constant pressure and δT is the energy difference between the convective eddy and the surrounding ambient medium. As the temperature decreases below ~5000 K, which corresponds to a mass $m < 0.6\ M_\odot$, H atoms recombine, n_{H_2} increases and so does $\bar{\kappa}$ through H_2 CIA (see above). The opacity increases by several orders of magnitude over a factor-of-2 change in temperature. On the other hand, the presence of molecules increases the number of internal degrees of freedom (vibration, rotation, electronic levels) and thus also c_p. These combined effects strongly favour the onset of convection in the optically thin ($\tau < 1$) atmospheric layers. This can be shown easily from a stability (Schwarzchild) criterion analysis. Flux conservation thus reads

$$\nabla(F_{rad} + F_{conv}) = 0 \tag{9}$$

i.e. no radiative equilibrium. The evolution of low-mass objects (low-mass stars, BDs, GPs) thus requires one to solve the complete set of transfer equations and to use consistent boundary conditions at the interface between the atmosphere and the interior structure profiles (Chabrier and Baraffe 1997, Baraffe *et al* 1995, 1997, 1998, Burrows *et al* 1997).

4. Screening factors and the lithium test

Since a BD, by definition, never reaches thermal equilibrium ($L \sim T\ \mathrm{d}S/\mathrm{d}t$), age is an extra degree of freedom, yielding an indeterminacy in the mass and/or age of an object for a given observed luminosity and/or temperature. An independent age indicator is thus needed. The presence of lithium in the atmosphere of a cool object provides such an indication. The signature of lithium absorption as a diagnostic for the sub-stellar nature of an object was first pointed out by Rebolo *et al* (1992) while the measure of lithium depletion as an age tracer was first used by Basri *et al* (1996).

The physics underlying the lithium test is rooted in dense-plasma physics and in the calculations of the so-called nuclear screening factors for the nuclear reaction rate.

Primordial ^{7}Li is destroyed through the nuclear reaction $^7\mathrm{Li} + \mathrm{p} \rightarrow 2^4\mathrm{He}$. The reaction rate R_0 (in $\mathrm{cm}^{-3}\ \mathrm{s}^{-1}$) in the vacuum is given by the usual Gamow theory rule $R_0 \propto \mathrm{e}^{-3\epsilon_0/kT}$ where ϵ_0 corresponds to the Gamow-peak energy for non-resonant reactions, which corresponds to the maximum probability for the reaction. However, as mentioned above, non-ideal effects dominate in the interior of BDs and lead to polarization effects in the plasma. These polarization effects due to the surrounding particles yield an enhancement of the reaction rate, as was first recognized by Schatzman (1948) and Salpeter (1954). The distribution of particles in the plasma reads

$$n(r) = \bar{n}\mathrm{e}^{-Ze\phi(r)/kT} \tag{10}$$

with

$$\phi(r) = \frac{Ze}{r} + \psi(r) \tag{11}$$

where $\psi(r)$ is the induced mean-field potential due to the polarization of the surrounding particles. This induced potential lowers the Coulomb barrier between the fusing particles and thus yields an *enhanced* rate in the plasma $R = ER_0$ where

$$E = \lim_{r\to 0}\left\{ g_{12}(r)\exp\left(\frac{Z_1 Z_2 e^2}{rkT}\right)\right\} \tag{12}$$

is the enhancement (screening) factor and $g_{12}(r)$ the pair distribution function.

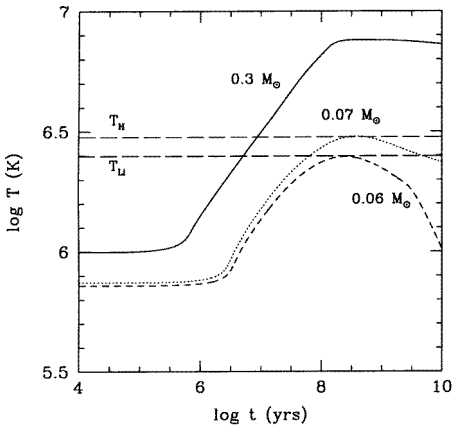

Figure 3. The central temperature as a function of age for three different masses: above, at the limit and below the hydrogen-burning minimum mass. $T_{\rm H}$ and $T_{\rm Li}$ indicate the hydrogen- and lithium-burning temperatures, respectively.

Under BD conditions, not only must *ionic* screening be included but so also must *electron* screening, i.e. $E = E_i E_e$. The two effects are of the same order ($E_i \sim E_e \sim$ a few) and must be included in the calculations for a correct estimate of the lithium-depletion factor $[\mathrm{Li}]_0/[\mathrm{Li}]$, where $[\mathrm{Li}]_0 = 10^{-9}$ denotes the primordial lithium abundance, to be obtained. This yields a lithium-burning minimum mass $m_{\rm Li} \sim 0.06\ M_\odot$ (Chabrier and Baraffe 1997), *below* the hydrogen-burning minimum mass, as illustrated in figure 3. After the common primordial deuterium-burning phase, which lasts $\sim 10^6$–10^7 years, the central temperature evolves differently, depending on the mass of the object. Note the strong age dependence of the lithium test: young *stars* with an age $t \lesssim 10^8$ years (depending on the mass) will exhibit lithium, whereas massive *brown dwarfs* within the mass range 0.06–0.07 $M_\odot$ older than $\sim 10^8$ years will have burned lithium. The measure of lithium depletion in the atmosphere of low-mass objects, inferred from the width of the Li I line at 6708 Å, as an age indicator, is illustrated in figure 4. This figure displays the evolution of a 0.075 $M_\odot$ object, the H-burning limit for solar abundances, in the I-band magnitude. The left-hand and right-hand diagonal solid lines correspond to 50% Li depletion ($[\mathrm{Li}]_0/[\mathrm{Li}] = 1/2$) and 99% Li depletion, respectively. Thus, for say 120×10^6 years, the inferred age of the Pleiades cluster, objects brighter than $M_I \sim 12.2$ will lie on the right-hand side of the 99%-depletion line and thus are predicted to show no lithium in their atmosphere and to be H-burning stars ($m \geqslant 0.075\ M_\odot$), whereas objects fainter than this magnitude will all show *some* lithium and all be brown dwarfs ($m < 0.075\ M_\odot$ for this age), with objects fainter than $M_I \sim 12.6$ predicted to have retained more than half of their primordial lithium abundance. The horizontal lines show the observed magnitudes of four different objects in the Pleiades, with available high-resolution spectra. All four confirm the theory, with no

lithium observed for PL10, about 50% depletion for PL13 and negligible or no depletion for Roq13 and Teide1. Different isochrones for different masses can be superimposed on the same diagram and analysed similarly. This illustrates convincingly the diagnostic power of lithium as a mass and age indicator for low-mass stars and brown dwarfs.

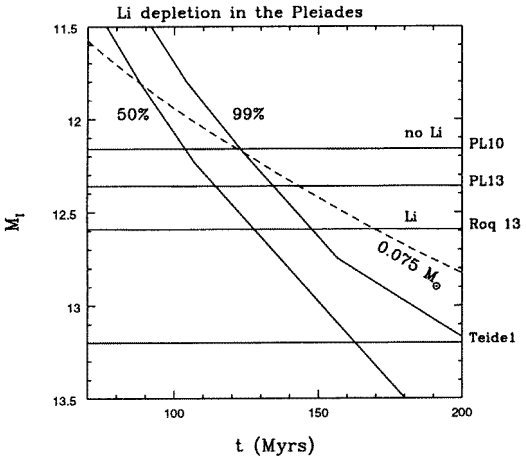

Figure 4. The evolution of the absolute magnitude M_I as a function of age. The dashed line corresponds to the hydrogen-burning minimum mass, whereas the diagonal solid lines correspond to the limits of 50% and 99% lithium depletion. The horizontal solid lines indicate the observed magnitudes of different low-mass objects.

5. Conclusions

As a conclusion to this paper, I will list a series of 'homework problems' related to BDs which illustrate the major problems to be addressed in this field in the near future and which correspond to different domains of physics or astronomy. This list is certainly not exhaustive.

(i) *Dense-matter physics*. As we have seen, tests on BD interiors can now be made directly in laboratories and the EOS of these objects can be probed by high-pressure experiments. More experiments are needed in the complex regime of H-pressure dissociation/ionization with several unanswered questions. Does the PPT really exist? Does it survive when 10% of the particles present are of helium? How does pressure ionization of H affect the dynamo process in BD and GP interiors?

(ii) *The star formation process*. Jeans stability analysis yields a minimum mass $m_{min} \sim 0.01\ M_\odot$, definitely in the BD domain (Silk 1977). Is this mass the BD minimum mass? Conversely, what is the maximum mass for planet formation? Does the Jeans criterion really apply for the formation of star-like objects? What is the BD *mass function* in the Galaxy?

(iii) *Evolution*. The evolution of BDs is not hampered by any adjustable parameter, like for example in the treatment of convection for a more massive star which develops an inner radiative core. The theory of BDs, and the comparison with observation, thus reflects the validity of the very physics entering the theory, both for the atmosphere and for the interior. This theory can be tested directly now by photometric and spectroscopic observations and must address new problems like, e.g., the diffusion process of grains in the atmosphere or

the magnetic field generation in active BDs. Conversely, the theory is now reliable enough to provide useful guidance for future observations.

(iv) *Galactic implications*. The mass-to-light ratios for BD, $(M/L)_{\rm BD} \gtrsim 10^4 (M/L)_{\odot}$, make BDs very promising candidates as regards explaining at least the baryonic missing mass. Even though present estimates of their contribution to the Galactic disc and halo mass seem to exclude this possibility (Chabrier and Méra 1997, Méra *et al* 1998a, b), the determination of their exact number and mass density in the Galaxy remains to be carried out accurately. Ongoing microlensing experiments sensitive to hour and day event durations and ongoing wide-field infrared projects (e.g. DENIS, 2MASS) will certainly help in 'nailing down' this issue.

BDs thus present a wide variety of areas of interest, from basic physics to Galactic implications, and should remain a very active field.

Acknowledgments

The results mentioned in this work to illustrate the physics of BDs arise from an ongoing collaboration with F Allard, I Baraffe and P H Hauschildt as regards the structure and the evolution of BDs, and with D Saumon as regards the EOS. My profound gratitude is extended to these colleagues for their contribution to this article.

References

Allard F, Alexander D, Hauschildt P H and Starrfield S 1997 *Annu. Rev. Astron. Astrophys.* **35** 137
Allard F, Hauschildt P H, Baraffe I and Chabrier G 1996 *Astrophys. J.* **424** 333
Baraffe I, Chabrier G, Allard F and Hauschildt P H 1995 *Astrophys. J.* **446** L35
——1997 *Astron. Astrophys.* **327** 1054
——1998 *Astron. Astrophys.* **337** 403
Basri G, Marcy G and Graham J R 1996 *Astrophys. J.* **458** 600
Borysow A, Trafton L, Frommhold L and Birnbaum G 1985 *Astrophys. J.* **296** 644
Burrows A and Liebert J 1993 *Rev. Mod. Phys.* **65** 301
Burrows A, Marley M, Hubbard W B, Lunine J I, Guillot T, Saumon D, Freedman R, Sudarsky D and Sharp C 1997 *Astrophys. J.* **491** 856
Ceperley D 1998 *J. Phys.: Condens. Matter* **10** at press
Chabrier G and Baraffe I 1997 *Astron. Astrophys.* **327** 1039
Chabrier G and Méra D 1997 *Astron. Astrophys.* **328** 83
Chabrier G, Saumon D, Hubbard W B and Lunine J I 1992 *Astrophys. J.* **391** 817
Collins G W *et al* 1998 *Science* at press
Da Silva L B *et al* 1997 *Phys. Rev. Lett.* **78** 483
Delfosse X *et al* 1997 *Astron. Astrophys.* **327** L25
Goldstein R E and Ashcroft N W 1985 *Phys. Rev. Lett.* **55** 2164
Gudkova T, Mosser B, Provost J, Chabrier G, Gautier D and Guillot T 1995 *Astron. Astrophys.* **303** 594
Hensel F 1998 *J. Phys.: Condens. Matter* **10** 11 395
Lunine J I, Hubbard W B and Marley M S 1986 *Astrophys. J.* **310** 238
Magro W R, Ceperley D M, Pierleoni C and Bernu B 1996 *Phys. Rev. Lett.* **76** 1240
Marley M S 1994 *Astrophys. J.* **427** L63
Marley M S, Saumon D, Guillot T, Freedman R, Hubbard W B, Lunine J I and Burrows A 1996 *Science* **272** 1919
Méra D, Chabrier G and Schaeffer R 1998a *Astron. Astrophys.* **330** 937
——1998b *Astron. Astrophys.* **330** 953
Nellis W J, Mitchell A C, van Thiel M, Devine G J and Trainor R J 1983 *J. Chem. Phys.* **79** 1480
Oppenheimer B R, Kulkarni S R, Nakajima T and Matthews K 1995 *Science* **270** 1478
Rebolo R, Martín E L and Magazzù A 1992 *Astrophys. J.* **389** 83
Rebolo R, Zapatero Osorio M R and Martin E L 1995 *Nature* **377** 83
Rogers F and Young D 1997 *Phys. Rev.* E **56** 5876

Ruiz M-T, Leggett S and Allard F 1997 *Astrophys. J.* **491** L107
Salpeter E E 1954 *Aust. J. Phys.* **7** 373
Saumon D, Bergeron P, Lunine L I, Hubbard W B and Burrows A 1994 *Astrophys. J.* **424** 333
Saumon D and Chabrier G 1991 *Phys. Rev.* A **44** 5122
——1992 *Phys. Rev.* A **46** 2084
Saumon D, Chabrier G, Wagner D J and Xie X 1998 *Phys. Rev. Lett.* submitted
Saumon D, Hubbard W B, Chabrier G and Van Horn H M 1992 *Astrophys. J.* **391** 827
Schatzman E 1948 *J. Physique Radium* **9** 46
Silk J 1977 *Astrophys. J.* **211** 638
Stevenson D 1991 *Annu. Rev. Astron. Astrophys.* **29** 163
——1998 *J. Phys.: Condens. Matter* **10** 11 227
Stevenson D and Ashcroft N W 1974 *Phys. Rev.* A **9** 782
Stevenson D J and Salpeter E E 1977 *Astrophys. J. Suppl.* **35** 221
Tsuji T, Ohnaka K and Aoki W 1996 *Astron. Astrophys.* **305** L1
Weir S T, Mitchell A C and Nellis W J 1996 *Phys. Rev. Lett.* **76** 1860
Wigner E and Huntington H B 1935 *J. Chem. Phys.* **3** 764